

Secondary frame action in concentrically braced frames designed for moderate seismicity: a full scale experimental study

Alper Kanyilmaz¹ 

Received: 21 October 2016 / Accepted: 18 November 2016 / Published online: 28 November 2016
© Springer Science+Business Media Dordrecht 2016

Abstract European seismic design codes do not take into account the strength and stiffness of the secondary frame action provided by bracing gusset plates of concentrically braced frames (CBFs). This is an attractive assumption for practicing engineers, as it provides simplifications during the analysis and design phases. However, when efficiency and economy are concerned, especially in low-to-moderate seismic regions, this normally neglected frame resource may be interesting to consider in design. Gusset plates can provide a certain degree of stiffness and strength following the bracing failure, and may even prevent global collapse. In particular, when the shear deformation demand of the braced cell remains limited, as in the case of low-to-moderate seismic actions, it may become reasonable to take this extra stiffness and strength into account. Ongoing research project RFSR-CT-2013-00022 MEAKADO investigated this phenomenon by means of experimental and numerical studies with the perspective of setting new inputs for the design rules of the future generation of Eurocodes. This paper presents the results of full scale tests performed inside this research project, which characterized resistance, stiffness, and ductility resources of CBF systems designed for moderate seismicity. The paper also quantifies the effective contribution of the frame action, provided by gusset plate connections, to the global performance of CBF frames.

Keywords Concentrically braced frames · Moderate seismicity · Secondary frame action · Gusset plate connections · Full scale tests · Steel frame reserve capacity

✉ Alper Kanyilmaz
alper.kanyilmaz@polimi.it

¹ Department of Architecture, Built Environment and Construction Engineering, ABC, Politecnico di Milano, Milan, Italy

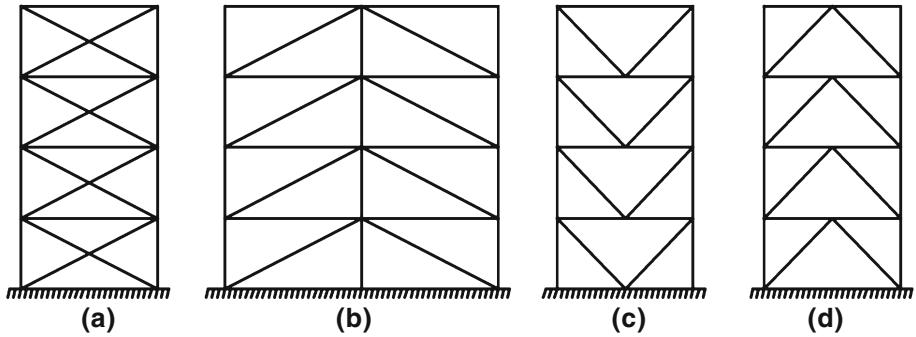


Fig. 1 Concentrically braced frame configuration types classified by EN1998-1-2004 (2004). **a** X-bracing, **b** N-bracing, **c** V-bracing, **d** inverted-V bracing

1 Introduction

Concentrically braced frame (CBF) configuration (Fig. 1) is very effective to resist horizontal loads. Indeed, 80–90% of the existing steel structures are laterally braced by CBF at least in one direction (Degée et al. 2015). Under earthquake actions, its high lateral strength and stiffness provide an abundant safety for steel buildings. For these structures, current European design recommendations define the seismic resistant system as a combination of primary (bracings) and secondary (non-structural walls, semi-rigid beam-to-column connections) seismic components. The resistant component is considered as “secondary”, when its total contribution to the lateral stiffness is less than 15% of all primary seismic components. In this case, Eurocodes allow designers to neglect the strength and stiffness of these parts in the seismic resistant system (EN1993-1-1-2005 2005a).

Despite even simple gusset plate connections may contribute to this secondary strength and stiffness capacity, at present they are not taken into account in design, and treated as

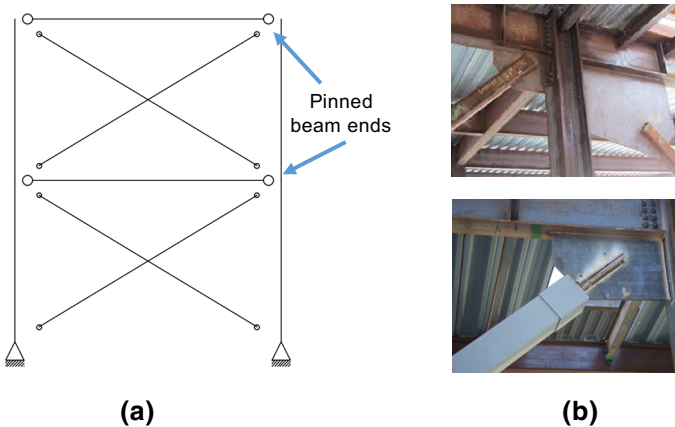


Fig. 2 Traditional CBF modelling with pinned beam ends. **a** CBF with pinned beam ends, **b** CBF with semi-rigid beam ends. Source <https://www.ecs.umass.edu/cee434/tour/ScienceSteel>

simple pinned joints (as shown in Fig. 2). This assumption is attractive for design engineers as it provides simplifications during the analysis and design phases. However, when efficiency and economy are concerned, especially in low-to-moderate seismic regions, this normally neglected frame resource may be economically interesting to consider due to the limited shear deformation demand of CBFs.

Current seismic code assumptions originate from the traditional focus of seismic engineering community on maximizing the building performance in the high-seismicity context. Application of the same assumptions to the low-to-moderate seismicity may not be economically feasible. This issue has been recently highlighted by several researchers worldwide (Gioncu and Mazzolani 2010; Stoakes 2012; Nelson et al. 2006; Kanyilmaz et al. 2013, 2015; Murty and Malik 2008; Reaveley and Nordenson 1990; Callister and Pekelnicky 2011; Han and Choi 2008; Kelly and Zona 2006; Pinto 2000). Specific assumptions for frame action tuned for low-to-moderate seismicity, can increase the global performance of CBF structures, and their design can be optimized (Gioncu and Mazzolani 2010). Several researchers studied the secondary frame contribution to CBF building performance designed for high seismicity (Hsiao et al. 2013; Málaga-Chuquitaype et al. 2014; Vargas and Bruneau 2008). For moderate seismicity, recent research exists, but limited to component based experimental activities (Stoakes and Fahnestock 2010). There are few recent studies that investigate the performance of beam-to-column shear and gusset plate connections (Stoakes 2012a; Yoo et al. 2008, 2009; Carter 2009) developed for US design practice. European design practice does not provide any specific procedure to design beam-to-column connections involving bracing gusset plates. Elghazouli et al. (2008) underlines the need to develop European guidelines on the design and detailing of recommended bracing connections for seismic resistance, by means of experimental research.

Uriz and Mahin (2008) investigated the contribution of beam-to-column connections involving gusset plates by means of full scale tests (Fig. 3). The specimen was designed according to high seismicity (ductile) approach (SCBF) of AISC Seismic Design Provisions (2010). Authors pointed out a considerable frame action developed by the beam-to-column gusset plate connections. This frame action contributed to the lateral load resistance of the specimen after braces buckled, carrying 30% of the peak lateral load

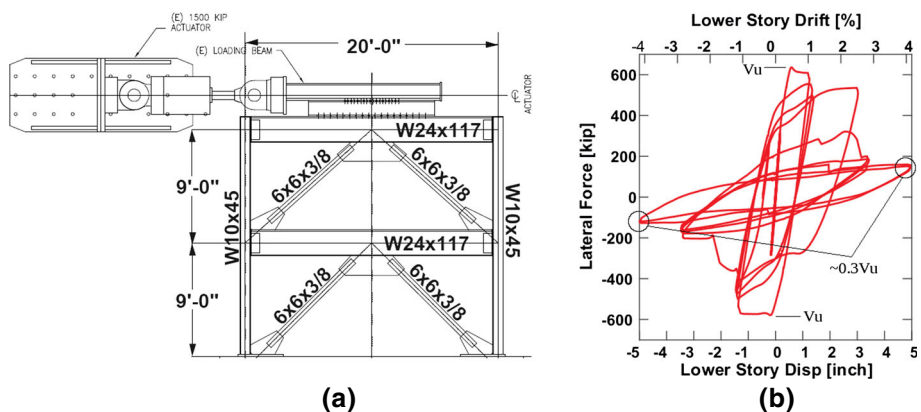


Fig. 3 Tests performed by Uriz et al. **a** Test specimen, **b** global horizontal load versus story drift

developed by whole braced specimen, an aspect which was not considered during design. This was a very interesting outcome for braced frames designed for high seismic actions.

Hines et al. (2009) underline the necessity to consider the steel frame design in moderate seismicity regions in a new manner. They propose an independent seismic design philosophy for low-ductility structures in moderate seismicity regions, specifically focusing on the reserve capacity concept, and its ability to improve collapse performance for chevron braced steel frames not specifically detailed for seismic resistance. Keeping the behavior factor small as possible ($R = 3$, according to American Standards), they try to exploit the energy dissipation characteristics of the gravity system which serves as reserve capacity, although this is not permitted by the current standards.

Aboosaber et al. investigated reserve capacity possessed by braced steel frames in the form of gravity framing and gusset plate connections, focusing on the welded bracings with tubular cross sections (Aboosaber et al. 2012). The semi-rigid joints forming a reserve moment frame prevented sideways collapse even when the bracings get damaged and fractured which means that primary lateral force resisting system is eliminated (Fig. 4). Authors proposed designing braced frames in low and moderate seismicity regions as moderate-ductility dual systems, which can improve the seismic behaviour of steel structures in these zones while keeping the design as simple as possible. Using this approach, moderate-ductility systems can achieve global ductility through coupling of a stiff braced and a flexible semi-rigid moment-resisting frame, on contrary to the high-ductility systems where the ductility is achieved mainly by means of plastic buckling and tensile yielding of bracings. In this way, even though the brittle CBF system fails, the flexible reserve system would possess sufficient strength, stiffness and ductility to prevent global collapse.

Stoakes and Fahnestock (2010) has studied beam-to-column connection flexural behaviour and seismic collapse performance of concentrically braced frames (Fig. 5). They performed tests at component level, and indicated as future research directions, the need of a validation by means of large-scale testing providing observations regarding the complex interaction between bracings, beams, columns, and connections.

In Japanese design practice, bracing systems are always combined with moment-resisting frames, and the global ductility parameters of braced frames depend also on the frame ductility (Marino et al. 2005). Japanese building code (BCJ 1997) classifies four moment-resisting frame (FA, FB, FC, FD), and three bracing classes (BA, BB, BC), letter “F” standing for frame, and “B” standing for bracing, whereas the letters A, B, C, D describes the ductility class (Table 1). The smallest behavior factor D_s value (0.25) stands for the most ductile frame type “FA” (Japanese behaviour factor “ D_s ” has smaller values for higher ductility, in contrast to the European behavior factor q). Ductility of BA, BB, BC

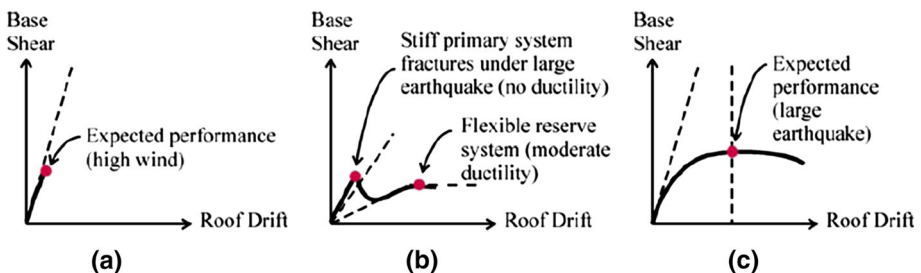


Fig. 4 Three design principles. **a** Low seismic, **b** moderate seismic, **c** high seismic (Aboosaber et al. 2012)

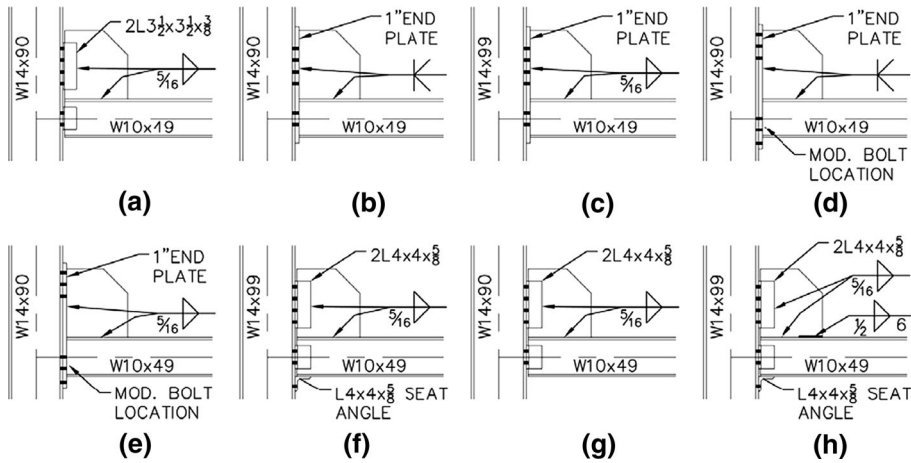


Fig. 5 Connection details studied by Stoakes and Fahnestock (2010). **a** CN1, **b** CN2, **c** CN3, **d** CN4, **e** CN5, **f** CN6, **g** CN7, **h** CN8 (With permission from ASCE)

Table 1 Behaviour factor “Ds” in Japanese seismic code (Marino et al. 2005) (With permission from Elsevier)

Type of MRF	Type of brace		Ductility increases ←				
	BA or $\beta = 0$	$\beta \leq 0.3$	BB $0.3 < \beta \leq 0.7$	$\beta > 0.7$	BC $\beta \leq 0.3$	$0.3 < \beta \leq 0.5$	$\beta > 0.5$
FA ↑ Ductility increases	0.25	0.25	0.30	0.35	0.30	0.35	0.40
FB	0.30	0.30	0.30	0.35	0.30	0.35	0.40
FC	0.35	0.35	0.35	0.40	0.35	0.40	0.45
FD	0.40	0.40	0.45	0.50	0.40	0.45	0.50

types are determined according to the bracing slenderness. For braced frames, “ D_s ” is modified by means of “ β ” parameter, which is the ratio between the shear sustained by bracings and the total braced frame. Ductility of braced frame types BB and BC increases with a higher frame participation, when the β values are smaller than 0.7 (i.e. 70% of the shear sustained by bracings), and 0.5 respectively. Arising from an essentially strong-seismicity approach, these threshold values can be considered as high, but it reflects very well the philosophy of exploiting the frame action in braced structures.

The literature study showed that most of the earthquake engineering research focused on applications for the regions exhibiting a high seismicity level, with the aim of maximizing the capacities of buildings in terms of energy dissipation and preventing brittle collapses. Very few research projects investigated the contribution of gravity systems to the lateral system in moderate seismic zones, mostly compatible to US standards. On the other hand, researchers worldwide acknowledge the necessity to find specific design strategies for the CBF structures designed for moderate seismicity. However, very few experimental evidence is available for the characterization of various resistance, stiffness, and ductility resources of braced frames designed for moderate seismicity, mostly limited to the experiments at a component level (e.g. testing only joints), or full scale tests investigating

CBFs designed for high seismic actions. There is not enough evidence to quantify the real performance of CBFs designed for moderate seismicity, and draw general conclusions.

European research project RFSR-CT-2013-00022 MEAKADO (Degée et al. 2015; Kanyilmaz 2015) investigates the possibilities to develop specific design methodologies for steel and steel–concrete composite structures in regions characterized by a low to moderate seismic activity, with an appropriate reliability level. It comprises a combination of experimental and numerical studies and aims to formulate proposals according to a pre-standard format in the perspective of further revisions of the design codes. This paper presents the results of full scale tests performed within this research project, which characterize resistance, stiffness, and ductility resources of CBF systems designed for moderate seismicity. The paper focuses on the frame action provided by gusset plate connections of CBF systems, and quantifies its contribution to the global performance of CBF frames designed for moderate seismicity.

2 Experimental program

Although the existing earthquake engineering literature focuses on the high-seismicity context, potential benefits of the secondary frame action of CBF structures have been recently emphasized for low-to-moderate seismicity. Yet, there is still not enough experimental evidence to quantify different aspects of this phenomena related to seismic performance of buildings designed for moderate earthquake actions. For this reason, full scale tests have been designed and performed as a task of the ongoing EU-RFCS MEAKADO project (Degée et al. 2015). From these experimental studies, recommendations for the design of concentrically braced frames in areas with moderate seismicity have been derived, and will be presented hereafter.

Test specimens represent a single storey frame extracted from a multi-storey structure, with dimensions corresponding to realistic full sizes of a building frame, yet limited by the testing facilities. 24 full scale cyclic tests have been performed with specimens of 1 level and 1 bay (2.6 m height and 4.3 m length), having three types of bracing profiles. Two types of test frames have been used:

- A moment resisting frame with semi-rigid beam-to-column connections (MRF) (Fig. 6a).
- A frame with ideally pinned connections (PC) (Fig. 6b).

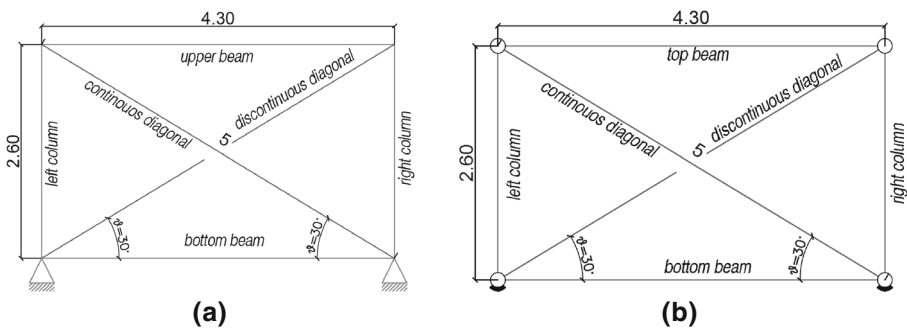


Fig. 6 Conceptual scheme of **a** MRF, Frame with semi-rigid joints and **b** pinned frame (measures in meters), frame with ideally pinned joints

In the first case (MRF), semi-rigid beam-to-column joints have been obtained by means of a gusset plate bolted both to the beams and columns. In the second case (PC), beam-to-column connections have been realized by steel pins that introduce rotational degree of freedom in the loading plane.

Figure 7 shows the construction drawings of the MRF and PC specimens. Beams and columns of these frames have been designed in such a way that they remain elastic at collapse limit state. In the tests, inelastic deformation is permitted and limited only to the bracings and their connections. Between MRF and PC specimens, the overall frame dimensions are kept equal about element inter-axes, so that comparison can be easily made between several tests. Gusset plates are designed in such a way that they can be bolted to the beam and column members of the test frame to allow an easy installation and replacement. After each test, gusset plates and bracing elements have been replaced.

Different bracing configurations have been tested. MRF specimen has also been tested without bracings, with and without gusset plates. The six configurations are described as follows (Fig. 8):

1. X-braced MRF specimens.
2. Single braced MRF specimens.
3. X-braced PC specimens.
4. Single braced PC specimens.
5. MRF specimens without bracings, with gusset plate connections.
6. MRF specimens without bracings and gusset plate connections.

The specimens have been designed according to 30-1-1 recommendations (EN1993-1-1-2005 2005a). Beam-to-column connections of MRF specimen have been designed using

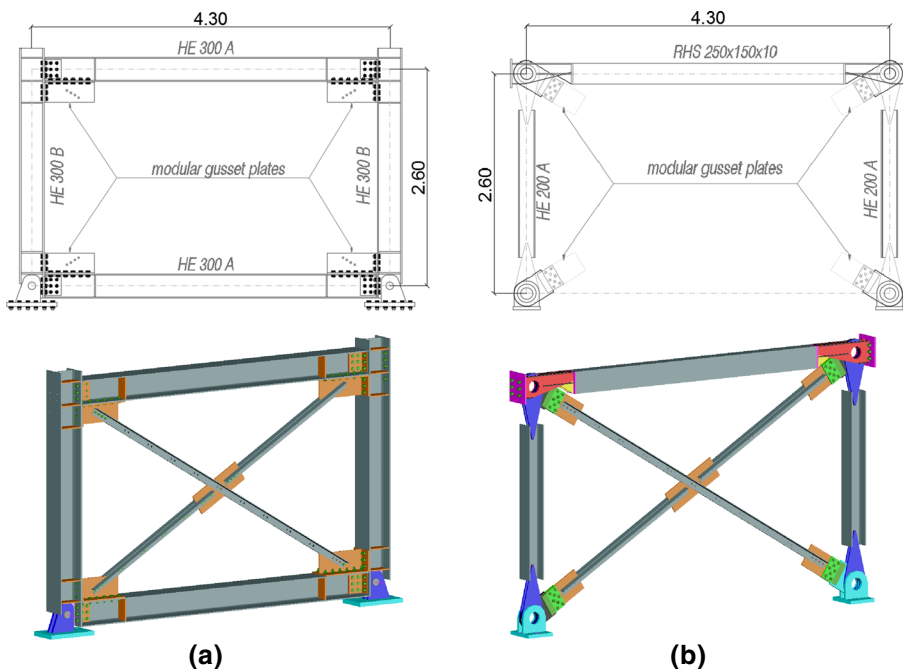


Fig. 7 Test frame drawings. **a** MRF with bracings, **b** PC with bracings

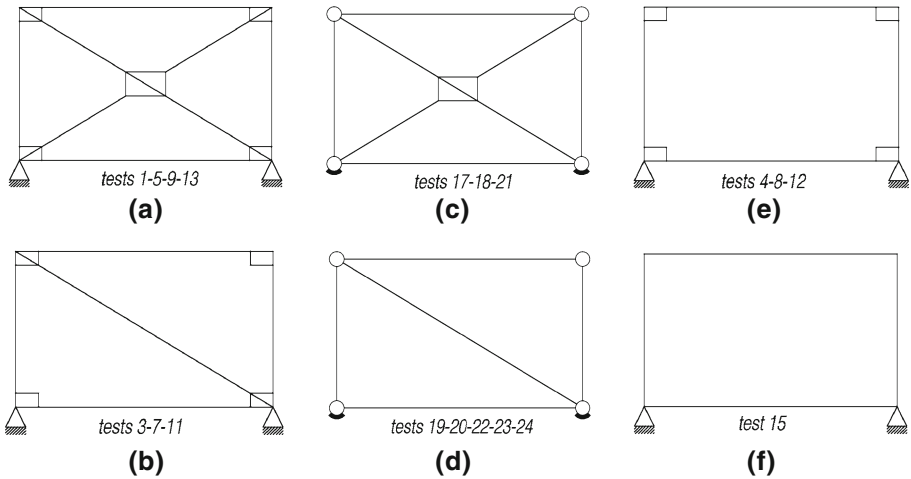


Fig. 8 Test configurations. **a** X-braced MRF, **b** single braced MRF, **c** X-braced PC, **d** single braced PC, **e** MRF with gusset plates, **f** MRF without gusset plates

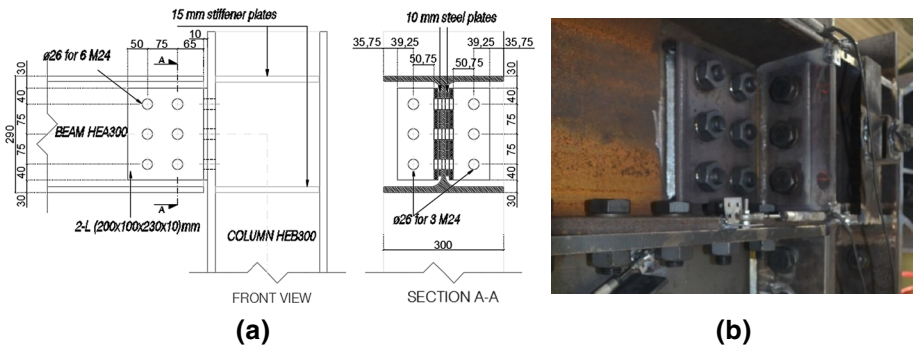


Fig. 9 Beam-to-column connections of MRF test frame. **a** Beam-to-column connection detail, **b** test specimen picture

double angle plates bolted both to the column flange and to the beam web, by means of $\Phi 24$ mm high strength bolts (Fig. 9). This connection type is not expected to have a significant flexural strength and stiffness, with a behaviour close to ideal pin. Therefore, it has been verified against the limit states of shear failure, block shear and bearing strength at the bolt holes.

Gusset plates connecting the bracing joints to the beam-to-column connections have been designed according to uniform force method (American Institute of Steel Construction 2010). They have been designed to avoid buckling under bracing compression loads so that the inelastic deformation is limited only to in-plane buckling of the bracing. Although plastic rotations of gusset plates can be desirable from structural point of view, in the case with double angle bracings, it causes out-of-plane buckling which would eventually damage non-structural components of the building. For moderate seismicity, preventing out-of-plane buckling can be more reasonable due to the low ductility demand.

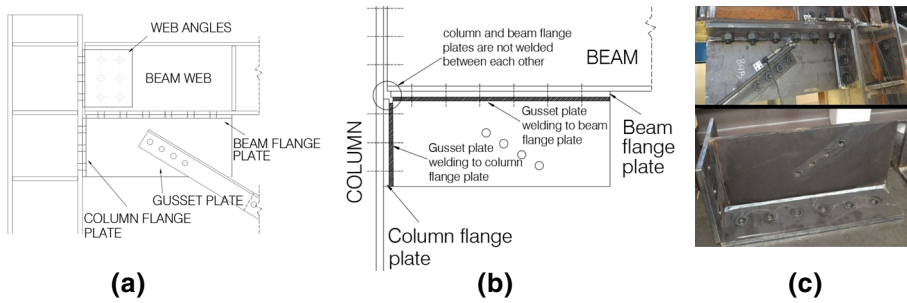


Fig. 10 Beam-to-column joint with gusset plate. **a** Beam-to-column joint, **b** welding detail of gusset plate, **c** test specimen

The gusset plates are welded to the steel plates which are bolted to the beam and column members. The column and beam flange plates are not welded between each other to avoid an extra rotational restraint in the joint (Fig. 10b). This detail was needed in the full-scale tests, to represent the behavior of typical gusset plate connections used in practice, where gusset plates are directly welded to the column and beam flanges.

Also in case of PC specimens, modular gusset plates have been realized, but in this case, the connection element has been hinged at the beam-to-column connection by means of high strength pins, releasing any flexural resistance for the frame. Gusset plates have been bolted to the “fork-type” pinned connection elements (Fig. 11).

Bracings are made of double angles arranged back-to-back by means of steel interconnectors, which is a typical bracing configuration widely used in Europe. Two angles were closely connected with steel plate interconnectors every 30–35 cm (compatible with the requirement of $15.i_{min}$ of EN1993-1-1 (EN 1993)), which permitted considering the angles as a single integral member under buckling. They are inclined by an angle $\theta = 30^\circ$ with the respect of the horizontal axis and have a theoretical length of 5.00 m. The following profiles have been tested:

- 2L-profile $60 \times 60 \times 8$ mm with 4M16 10.9 pre-tensioned bolts.
- 2L-profile $70 \times 70 \times 7$ mm with 4M20 10.9 pre-tensioned bolts.
- 2L-profile $80 \times 80 \times 8$ mm with 4M20 10.9 pre-tensioned bolts.

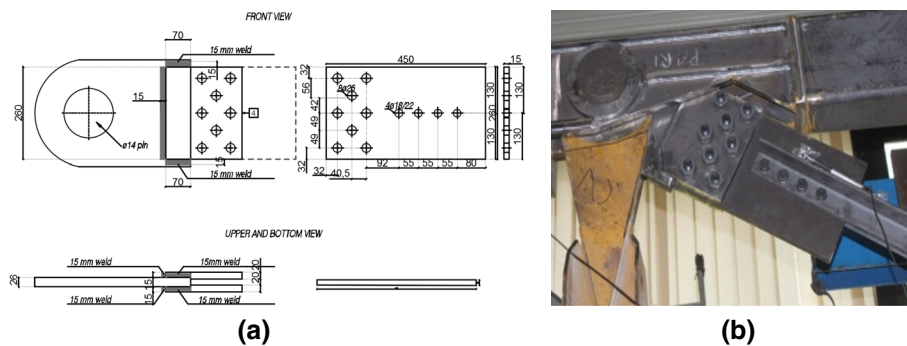


Fig. 11 Gusset plate connection of PF test frame. **a** “Fork type” gusset plate connection element, **b** test specimen picture

Table 2 Geometric characteristics of the diagonal connections

Profile	L (mm)	T (mm)	E_1 (mm)	e_2 (mm)	p_1 (mm)	d_0 (mm)	$t_{int.}$ (mm)	A (mm)
2L80 × 80 × 8	80	8	30	40	55	22	15	2450
2L70 × 70 × 7	70	7	30	30	55	22	15	1880
2L60 × 60 × 8	60	8	30	28	55	18	15	1805

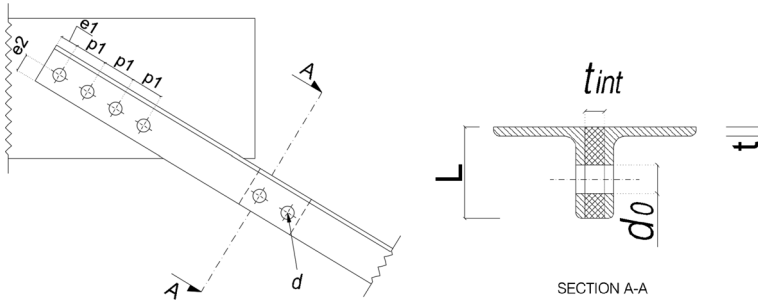


Fig. 12 Bracing connection detail



Fig. 13 Samples extracted from angular profiles of the braces for tensile tests

Table 2 shows the geometrical properties of the bracing profiles with reference to Fig. 12.

Mechanical properties of the steel used for the columns, beams, bracings and the connection elements have been evaluated by means of uni-axial tensile tests (Fig. 13). Table 3 reports the mechanical properties obtained from these tests.

All bracing connection bolts were pre-loaded according to the indications of EN1090-2 (UNI 1090). Combined method has been used, which consists a first tightening phase of the bolts by imposing a torque moment equal to 75% of the pre-load, and a second phase in which the nut is rotated with an additional angle as a function of the total thickness to be tightened (including the thickness of the washers). Table 4 summarizes the values calculated for the two types of bolts.

Table 3 Mechanical properties of the steel

Structural elements	Profile	Steel mechanical properties				
		Steel type	Design		Tensile test	
			f_y (Mpa)	f_u (Mpa)	f_y (Mpa)	f_u (Mpa)
Beam	HE 300 A	S355JR	355	510	375	547
Column	HE 300 B				362	559
Web connection	Double angle	S275JR	275	430	365	489
Diagonal	2L60 × 60 × 8				340	465
Diagonal	2L70 × 70 × 7				336	479
Diagonal	2L80 × 80 × 8				349	462
Gusset plates	Rectangular plate				387	517

Table 4 Tightening combined method: initial applied torque

Bolt	d (mm)	Resistance class	f_{ub} (N/mm ²)	A_{res} (mm ²)	$F_{p,C}$ (EN1090-2)	k	Mr (EN1090-2) (N*m)	Initial torque 75% M_r (N*m)	Additional rotation [°] $t < 32$
M16	16	10.9	1000.00	157.00	109.90	0.13	228.60	171.44	60
M20	20	10.9	1000.00	245.00	171.50	0.13	445.90	334.43	60

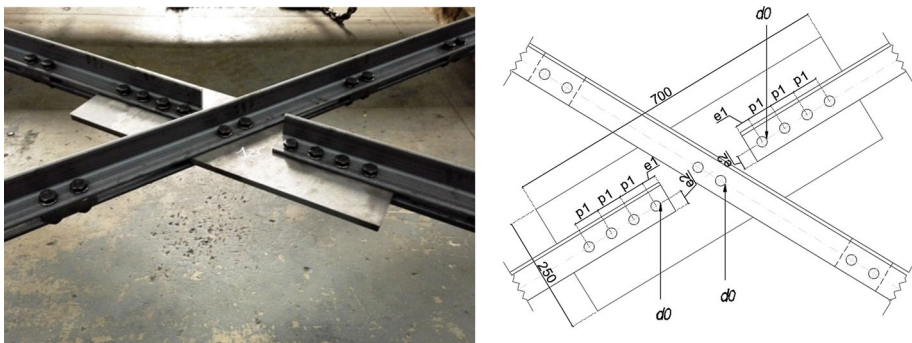


Fig. 14 Steel mid-plate of the bracing system

The bracings in X-type-configuration have been bolted to a steel mid-plate of 15 mm thickness, made of S275JR (Fig. 14).

Design parameters and results are shown in Table 5. In the table, S60, S70, S80 refer to the single bracing diagonals, and X60, X70, X80 refer to the X-bracing specimens. Bracing joints are designed according to EN1993-1-8 rules (EN1993-1-1-2005 2005b), without taking into account any dissipative design concept of EN1998 (EN1998-1-2004 2004). This “non-compliance to the capacity design criteria” is shown by means of C_R parameter, which is the ratio between joint resistance (R_d) and the section resistance with over-

Table 5 Bracing joint design parameters and results

Definition	Unit	S60 4M16	S70 4M20	S80 4M20	S60 4M16	S70 4M20	S80 4M20
Partial factor for resistance	γ_0	1	1	1	1	1	1
Partial factor for instability	γ_1	1	1	1	1	1	1
Partial factor for fracture	γ_2	1.25	1.25	1.25	1.25	1.25	1.25
Yield strength	f_y	275	275	275	275	275	275
Ultimate strength	f_u	430	430	430	430	430	430
Elastic modulus	E	210,000	210,000	210,000	210,000	210,000	210,000
Area of profile	A	1792	1862	2432	1792	1862	2432
Net area of profile	A_{net}	1504	1554	2080	1504	1554	2080
Minimum inertia	I_{min}	59.37	86.4	147.46	59.37	86.4	147.46
Effective length factor	k	0.9	0.9	0.9	0.45	0.45	0.45
Length	L	5	5	5	5	5	5
Effective length	L_{er}	4.5	4.5	4.5	2.25	2.25	2.25
Non-dim slenderness	$\bar{\lambda}$	2.85	2.41	2.11	1.42	1.20	1.05
Slenderness	λ	247.23	208.90	182.75	123.61	104.45	91.37
Min. Radius of gyration	i_{min}	1.82	2.15	2.46	1.82	2.15	2.46
Slenderness to determine $\bar{\lambda}$	λ_1	86.80	86.80	86.80	86.80	86.80	86.80
Imperfection factor	α_{LT}	0.34	0.34	0.34	0.34	0.34	0.34
Value to determine χ	ϕ	5.01	3.77	3.04	1.72	1.39	1.20
Reduction factor	χ	0.11	0.15	0.19	0.37	0.48	0.56
Bolt hole diameter	d_0	18	22	22	18	22	22
Section thickness	t	8	7	8	8	7	8
<i>Profile checks</i>							
Net section resistance	$N_{u,Rd}$	466	481	644	466	481	644
Section resistance	$N_{pl,Rd}$	493	512	669	493	512	669
Resistance with over-strength	$N_{pl,ov}$	678	704	920	678	704	920

Table 5 continued

Definition	Unit	S60 4M16	S70 4M20	S80 4M20	S60 4M16	S70 4M20	S80 4M20
Euler buckling load:							
N_{cr}	kN	61	88	151	243	353	603
Buckling resistance load							
$N_{buc,Rd}$	kN	54	77	128	183	244	377
<i>Joint checks</i>							
Bearing resistance							
$F_{b,Rd}$	kN	630	531	607	630	531	607
Shear resistance							
$F_{v,Rd}$	kN	502	784	784	502	784	784
Block tearing resistance							
$V_{eff,Rd}$	kN	440	378	459	440	378	459
Shear over-strength							
$F_{v,Rd}/F_{b,Rd}$	kN	0.80	1.48	1.29	0.80	1.48	1.29
Overstrength ratio $R_d/N_{pl,ov}$							
C_R		0.65	0.54	0.50	0.65	0.54	0.50

Table 6 Expected yielding sequence of specimens

Specimen	C_R	$\bar{\lambda}$	Ultimate resistance sequence				$F_{v,Rd}/F_{b,Rd}$
S60 4M16	0.65	2.85	Plastic buckling	Block tearing	Net section	Shear	0.80
S70 4M20	0.54	2.41	Plastic buckling	Block tearing	Net section	Bearing	1.48
S80 4M20	0.50	2.11	Plastic buckling	Block tearing	Bearing	Net section	1.29
X60 4M16	0.65	1.42	Plastic buckling	Block tearing	Net section	Shear	0.80
X70 4M20	0.54	1.25	Plastic buckling	Block tearing	Net section	Bearing	1.48
X80 4M20	0.50	1.09	Plastic buckling	Block tearing	Bearing	Net section	1.29

strength ($N_{pl,ov}$ of Eq. 1 with reference to EN1998-1-1 (EN1998-1-2004 2004)). Shear over-strength ($F_{v,Rd}/F_{b,Rd}$) has been estimated as a ratio between design shear and bearing resistance calculated according to EN1998-1-1 (EN1998-1-2004 2004) clause 6.5.5. The seismic requirement of 1.2 in this case has not always been considered.

$$N_{pl,ov} = 1.1\gamma_{ov}N_{pl,Rd} \quad (1)$$

where

R_d : $\min(F_{v,Rd}; F_{b,Rd}; N_{u,Rd}; V_{eff,Rd})$ with reference to Table 5.

$N_{pl,Rd}$: plastic resistance of the connected dissipative member based on the design yield stress of the material.

γ_{ov} : Over-strength factor (1.25).

C_R : $R_d/N_{pl,ov}$.

The specimens are designed so that first yielding mechanism is the plastic compression buckling, which is followed by the joint block tearing. Net section yielding is the next phenomena in the sequence for S60, S70, X60 and X70 specimens, while it is the bolt hole yielding due to bearing for the S80 and X80 specimens. All specimens except for S60 and X60 satisfy the 1.20 shear strength rule. None of the specimens satisfies capacity design rule, S60 and X60 are being the closest to achieve the requirement with 0.65 (Table 6).

Tests have been performed in “Laboratorio Prove Materiali” of Politecnico di Milano, from 11th February to 29th April of 2016. Test frame components are shown and listed in Fig. 15. In all tests, cyclic loading has been applied in correspondence to the top joint of right-side column by means of a short beam, transferring the force from the electromechanical actuator, which has a tension/compression capacity of 1000 KN, and a total stroke of 600 mm. Test specimens have been restrained out-of-plane. A displacement controlled loading protocol has been used. The tests have been performed in a quasi-static regime with an application of the displacement at a speed of 0.4 mm/s. ECCS loading protocol has been modified to obtain information at small displacement amplitude increment. Effect of gravity loads has been considered non-influent on the parameters under examination, therefore they have not been applied. Applied global horizontal load has been measured by means of a load cell attached to the loading jack. All the displacements have been measured at various locations of the specimens by means of displacement transducers (LVDT).

Axial deformations have been measured by means of strain gauges. 3-wire strain gauges with FLA-6-350-11-3LT model, manufactured by Tokyo Sokki Kenkyujo Co., with a resistance of 350 Ω , 6 mm grid length and a gauge factor equal to 2.12 have been used. Four strain gauges have been placed at bracing cross sections to calculate axial forces (Fig. 16). Positions of the strain gauges have been kept distant from the possible plastic hinge locations throughout the bracing elements.

The specimen photos are shown in Fig. 17.

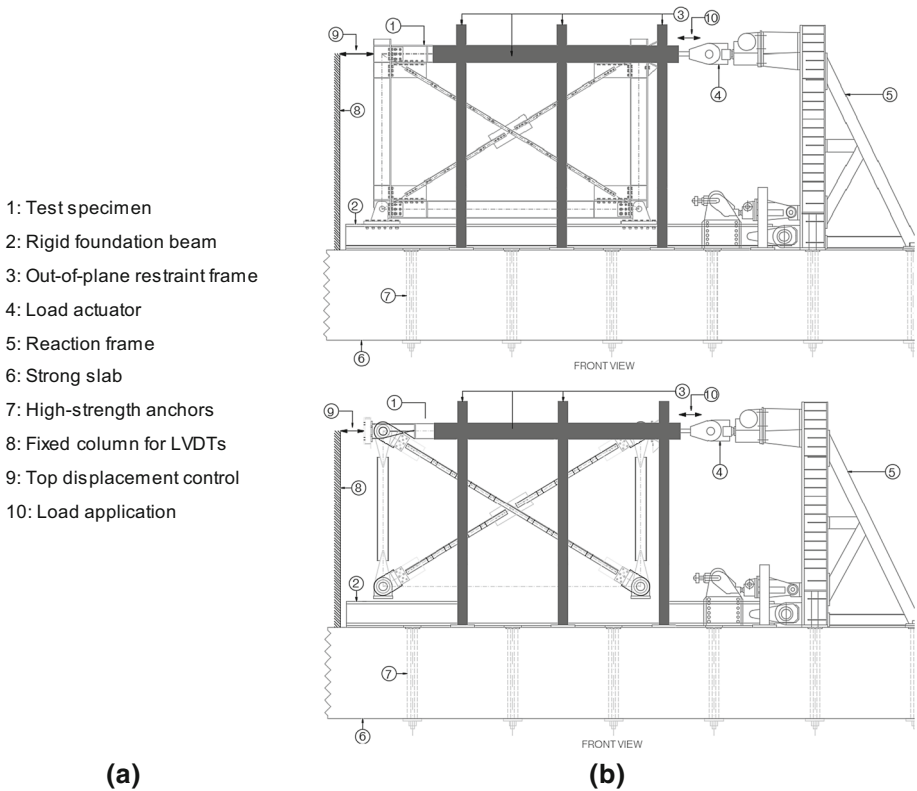


Fig. 15 Test set-up. **a** Legend, **b** test set-up for MRF (*top*) and PC (*bottom*) specimens

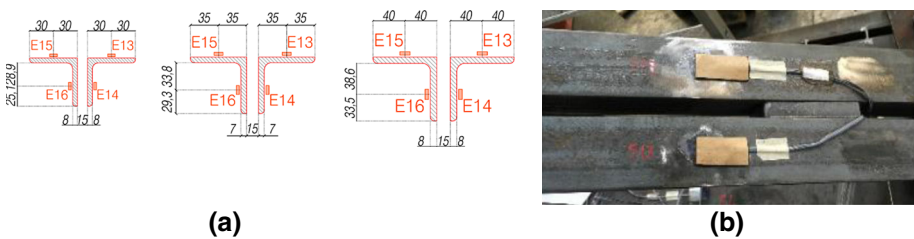


Fig. 16 Strain gauge positions at bracing cross section. **a** Exact positions of strain gauges, **b** example from a specimen

Final test program is summarized in Table 7, with the codes used in this paper.

3 Analysis of the test results

In CBF structures, “frame action” naturally exists in the form of beam-to-column shear connections and gusset plate connections of braces. Gusset plate connections provide an extra stiffness and strength engaging the beam and column by means of a welded plate to

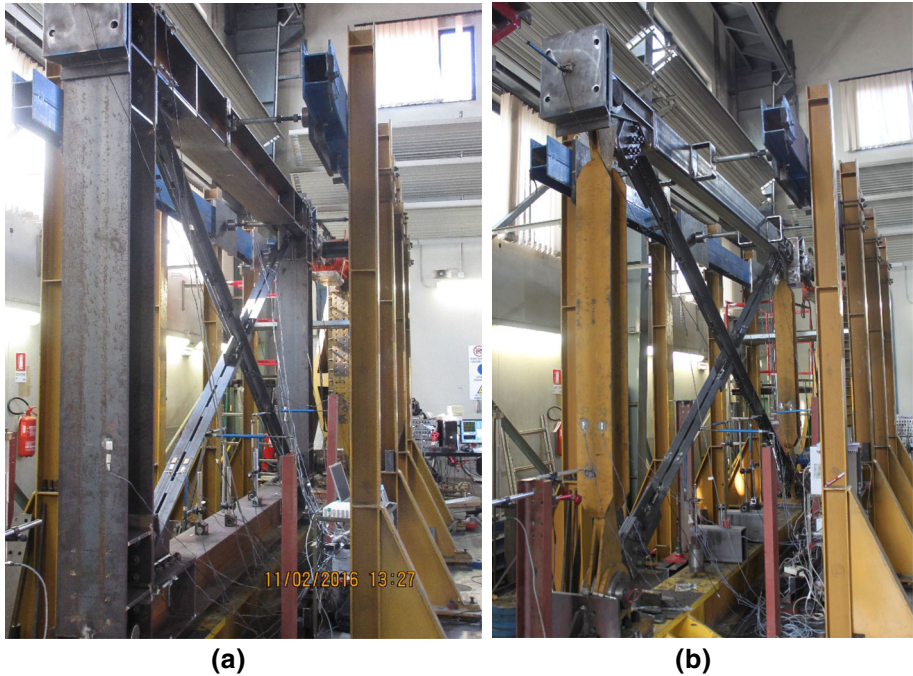


Fig. 17 Pictures of the test specimens. **a** MRF test specimen, **b** PC test specimen

which the concentric bracing is connected (Fig. 18). This may be a valuable resource as a secondary system to increase global resistance and ductility, and eventually prevent collapse, providing a certain degree of stiffness and strength following the bracing yielding and failure.

Despite even simple gusset plate connections may contribute to this “extra” strength and stiffness capacity in CBF systems, in European design practice these connections are normally designed as simple pinned joints. Several researchers have highlighted the fact that these connections may provide significant strength and stiffness, though only a few experimental studies have been carried out at global level to quantify them (Stoakes and Fahnestock 2010; Uriz and Mahin 2008; Kishiki et al. 2008). In this section, by means of the cyclic tests performed on the specimens schematized in Fig. 19, the secondary frame action has been quantified for the moderate-seismicity context.

Testing these specimens allowed the following investigations:

- Global behaviour of braced frames has been investigated by means of tests “a” (double bracing MRF specimens) and “b” (single bracing MRF specimens).
- Global elastic–plastic capacity assessments have been made by single bracing specimens and the double bracing specimen with slender bracings.
- Global stiffness assessments have been made by two double bracing specimens with less slender bracings.
- Test types “e” and “f” allowed the assessment of the frame action provided by gusset plates and beam-to-column shear connections.
- Test types “c” and “d” allowed the assessment of bracing behaviour thanks to idealized pin connections for bracing ends and beam-to-column joints.

Table 7 Global test program

Test no.	Bracing profile	Bracing connection	Frame connection	Configuration	Test code
1	2L60 × 60 × 8	4M16	MRF	X bracing, 50% Prestressed joints	X60-MRF_NP
2	2L60 × 60 × 8	4M16	MRF	X bracing no pres—No mid connection	X60-MRF-S
3	2L60 × 60 × 8	4M16	MRF	Single diagonal	S60-MRF
4	No bracing	–	MRF	MRF only	MRF
5	2L70 × 70 × 7	4M20	MRF	X bracing	X70-MRF
6	2L70 × 70 × 7	4M20	MRF	X bracing—No mid connection	X70-MRF-S
7	2L70 × 70 × 7	4M20	MRF	Single diagonal	S70-MRF
8	No bracing	–	MRF	MRF only	MRF
9	2L80 × 80 × 8	4M20	MRF	X bracing	X80-MRF
10	2L80 × 80 × 8	4M20	MRF	X bracing—No mid connection	X80-MRF-S
11	2L80 × 80 × 8	4M20	MRF	Single diagonal	S80-MRF
12	No bracing	–	MRF	MRF only	MRF
13	2L60 × 60 × 8	4M16	MRF	X bracing with prestress	X60-MRF
14	No bracing	–	MRF	MRF only	MRF
15	No bracing	–	MRF	MRF only, No gusset plate	MRF_NG
16	No bracing	–	MRF	MRF only	MRF
17	2L60 × 60 × 8	4M16	PC	X bracing	X60-PC
18	2L70 × 70 × 7	4M20	PC	X bracing	X70-PC
19	2L70 × 70 × 7	4M20	PC	Single diagonal	S70-PC
20	2L80 × 80 × 8	4M20	PC	Single diagonal	S80-PC
21	2L80 × 80 × 8	4M20	PC	X bracing	X80-PC
22	2L80 × 80 × 8	4M20	PC	Single diagonal	S80-PC
23	2L60 × 60 × 8	4M16	PC	Single diagonal	S60-PC
24	2L70 × 70 × 7	4M20	PC	Single diagonal, 50% Prestressed joints	S70-PC-NP

MRF Moment resisting frame, *PC* Frame with pinned connections

Sign convention of load application is shown in Fig. 20a. Base shear is obtained from the load cell attached to the actuator, while global interstorey-drift has been calculated from the LVDT measurements obtained at the top node displacement with the following formula (Fig. 20b):

$$IDR[\%] = \frac{\delta}{h} \times 100 \quad (2)$$

Figure 21 compares the full global behavior of four test specimens with different bracing elements. S60, S70, S80, X60 represent respectively the three specimens with single diagonals (respectively with 2L60 × 60 × 8, 2L70 × 70 × 7, 2L80 × 80 × 8 bracing profiles), and a double diagonal specimen with relatively high slenderness (2L60 × 60 × 8). Continuous (black) hysteresis curve shows the global force–

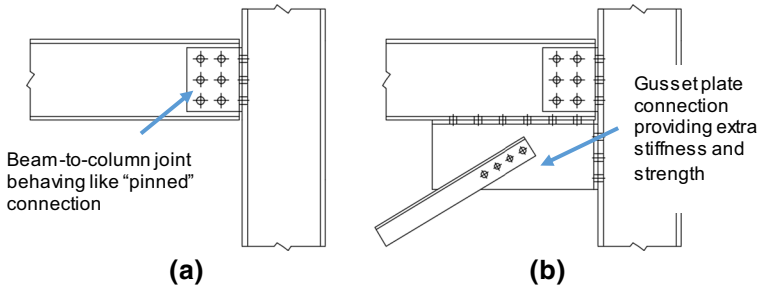


Fig. 18 Beam-to-column connections with and without bracing gusset plate. **a** without gusset plate, **b** with gusset plate

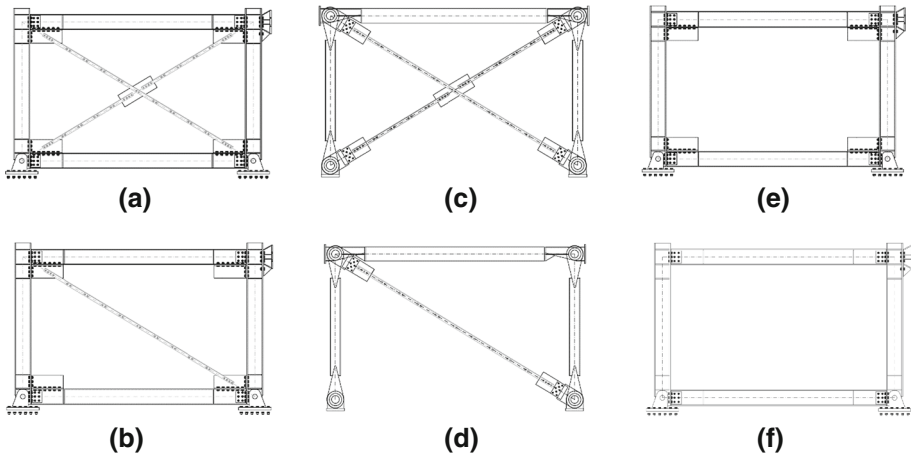


Fig. 19 Test configurations. **a** X-braced MRF (n. 1-5-9-13), **b** single braced MRF (n. 3-7-11), **c** X-braced PC (n. 17-18-21), **d** single braced PC (n. 19-20-22-23-24), **e** MRF with gusset (n. 4-8-12), **f** MRF without gusset (n. 4-8-12)

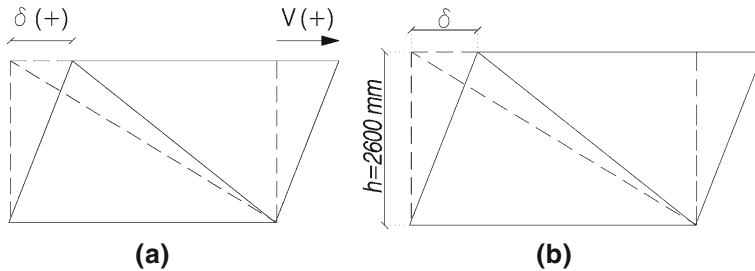


Fig. 20 Calculation of global interstorey drift. **a** Sign convention, **b** calculation of global interstorey drift

displacement behavior of the braced frame with single diagonal, drawn until bracing failure, while the dashed-line (blue) hysteresis curve shows the global force–displacement behavior of the MRF frame without bracings. The MRF specimen without bracings has been pushed until large drifts to simulate the performance of the braced frame after a total

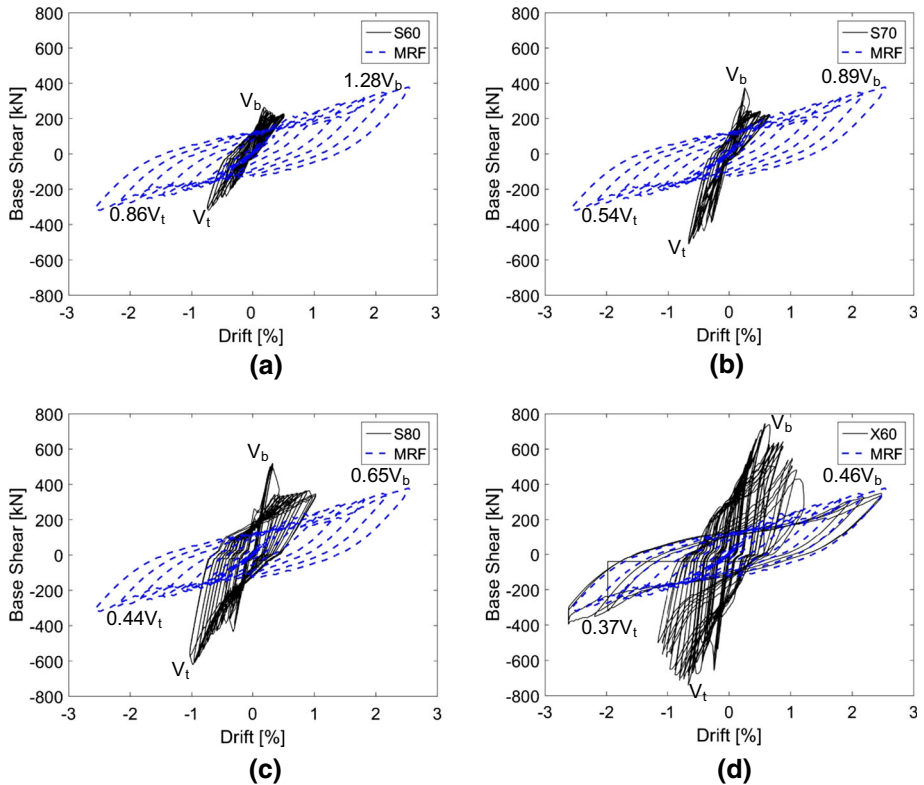


Fig. 21 Global behaviour of test specimens. **a** S60-MRF versus MRF (test types “b” and “e”), **b** S70-MRF versus MRF (test types “b” and “e”), **c** S80-MRF versus MRF (test types “b” and “e”), **d** S60-MRF versus MRF (test types “b” and “e”)

collapse of bracings. In all tests, secondary frame action could sustain a significant portion of the peak base shear.

Capacity of each specimen following the bracing failure is reported in Table 8, where:

- V_b Peak base shear (positive)
- V_t Peak base shear (negative)
- V_{fb} Peak base shear of MRF specimen in the same direction with V_b at 2% drift

Table 8 Peak base shear reached in the tests

	V_b (KN)	V_t (KN)	V_{fb}/V_b	V_{ft}/V_t
60S-MRF	264	−319	1.28	0.86
70S-MRF	376	−511	0.89	0.54
80S-MRF	520	−622	0.65	0.44
60X-MRF	740	−742	0.46	0.37
V_{fb} (KN)	337			
V_{ft} (KN)		−275		

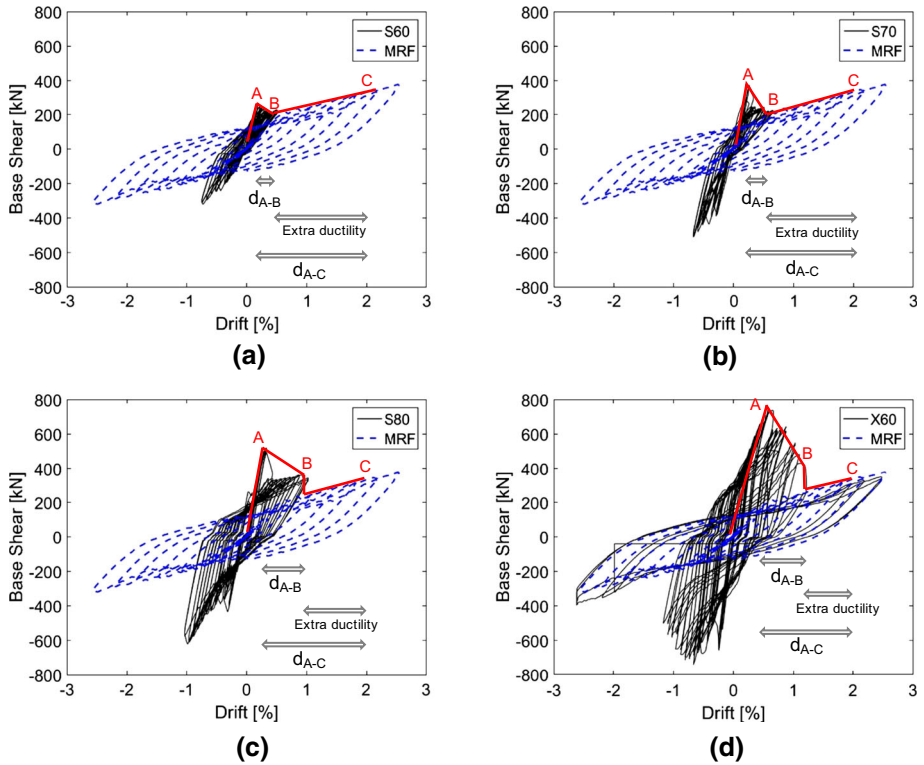


Fig. 22 Ductility resources of specimens. **a** S60-MRF specimen (test types “b” and “e”), **b** S70-MRF specimen (test types “b” and “e”), **c** S80-MRF specimen (test types “b” and “e”), **d** S60-MRF specimen (test types “b” and “e”)

V_{ft} Peak base shear of MRF specimen in the same direction with V_t at 2% drift

During post-buckling stage, specimens continued to have significant strength and stiffness. Figure 22 describes three points on the global behaviour of specimens:

- “A” Global lateral resistance when the buckling resistance of bracing reached
- “B” Minimum global lateral resistance during the post buckling stage
- “C” Global lateral resistance of the frame at 2.0% inter-storey drift

Table 9 Base shear and drift values at various points (A, B, C)

	V_A (kN)	IDR _A (%)	V_B (kN)	IDR _B (%)	V_C (kN)	IDR _C (%)	POST-RES (%)	FRAME-RES (%)	$\bar{\lambda}$
60S-MRF	264	0.19	212	0.40	337	2.00	80	127	2.85
70S-MRF	376	0.26	225	0.67	337	2.00	59	89	2.41
80S-MRF	520	0.33	347	0.98	337	2.00	67	65	2.11
60X-MRF	740	0.65	430	1.16	337	2.00	58	46	1.42

Numerical values corresponding to these points are summarized in Table 9 with the following parameters:

$V_{(A,B,C)}$	Global base shear
$IDR_{(A,B,C)}$	Global inter-storey drift ratio (%)
POST-RES	Ratio between the specimen's minimum post buckling and buckling resistance: V_B/V_A
FRAME-RES	Ratio between the specimen's frame-only (at 2% IDR) and the buckling resistance: V_C/V_A
$\bar{\lambda}$	Non-dimensional slenderness defined in Sect. 2

Ultimate resistance of the specimens was comparable to their buckling resistance. This means that even when the bracings were in the post-buckling stage, significant resistance was provided by the secondary frame alone. Ratio between the resistance provided by the braced frame with buckled diagonals and the buckling resistance changed between 58 and 80% (Table 9). When the bracings were largely damaged (at incipient collapse stage corresponding to 2% inter-storey drift), only secondary frame action could provide 46 to 127% of lateral resistance of the braced specimens. In case of S60-MRF specimen, the base shear has been increased and even reached values larger than the bracing buckling resistance, within the following cycles.

In all cases, when the bracings were completely damaged due to connection fractures, the moment resisting frame with semi-rigid joints provided an extra capacity. Thanks to this frame back-up, specimens continued to deform reaching large drifts (around 2.5%) with not too large but remarkable resistance and stiffness. Figure 23 shows the specimen X60 before and after section fracture.

Table 10 reports the global ductility provided by bracings-only, and the whole specimen, by means of the following parameters:

d_{A-B}	Ductility provided by bracing under compression (IDR_B/IDR_A)
d_{A-C}	Overall ductility (IDR_C/IDR_A)

Such a comparison [made with reference to the work of Aboosaber et al. (2012)], confirms that although the CBF systems are known to have limited ductility, when the frame action is able to provide sufficient strength and deformability, the overall ductility reaches important values. With the most slender diagonal (2L60 × 60 × 8) the overall ductility is more than three times the ductility provided by bracings. This significant frame action was mainly due to beam-to-column gusset-plate connections. This is seen in

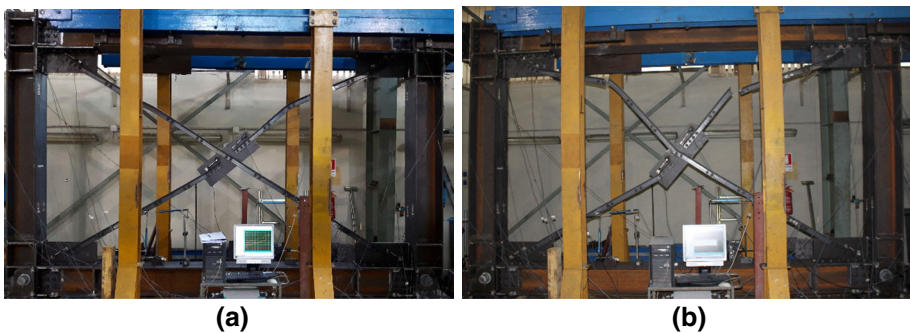


Fig. 23 Specimen X60 during post buckling and after bracings' complete failure. **a** during post-buckling, **b** after both bracings completely fractured

Table 10 Ductility provided by braced frame and overall ductility including frame reserve

	d_{A-B}	d_{A-C}	d_{A-C}/d_{A-B}	$\bar{\lambda}$
S60-MRF	2.11	10.53	4.99	2.85
S70-MRF	2.58	7.69	2.98	2.41
S80-MRF	2.97	6.06	2.04	2.11
X60-MRF	1.78	3.08	1.73	1.42

Fig. 24c, where the global base shear- inter storey drift behavior of the MRF specimen with and without gusset plates have been compared. In this case, 75% percent of the elastic stiffness, and the 79% of the ultimate resistance (at 2% drift) are provided by the gusset plate connections.

The source of the beam-to-column ductility is based on a combination of the inelastic deformations of T-stub connection between the gusset plate and the column (Fig. 25) and the web angles connecting the beam web to the column flange (Fig. 26).

Figure 27 shows comparisons between the global behavior of PC and MRF specimens with single diagonal profiles. The contribution of secondary frame action to global resistance is much more significant when the bracings are compressed. This global resistance increase is caused by the combination of two effects: semi-rigid beam end joints with gusset plates and reduced effective slenderness of bracings. The latter effect is due to the fact that in PC specimens the bracings and beam-ends are perfectly pinned, while in MRF specimens their boundary conditions can be considered as semi-rigid, with a rotational stiffness. Unquestionably, ideally pinned conditions result in higher effective slenderness, which is far from the reality. When the bracings are under tension, the effect of bracing boundary condition disappears on the global resistance capacity, and such capacity is affected only by the partial strength of the gusset plate beam-to-column connections. In this case, the influence of the frame effect decreases with decreasing the bracing slenderness. Figures 28 and 29 compare the global stiffness of MRF and PC specimens.

Table 11 reports the global stiffness values obtained in all tests, with following parameters:

$\bar{\lambda}$ Non-dimensional slenderness defined in Sect. 2

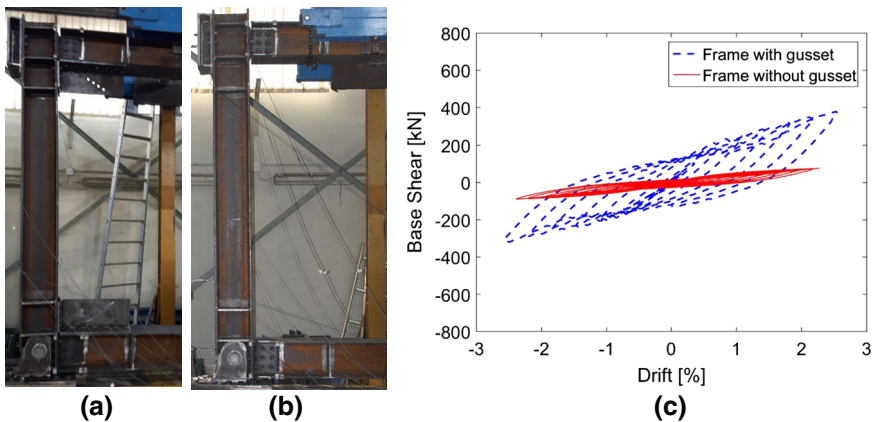


Fig. 24 Comparison between MRF specimens with and without gusset plate connections. **a** MRF with gusset plate connection, **b** MRF without gusset plate connection, **c** global base shear-drift behavior of the MRF specimen with and without gusset plate connections

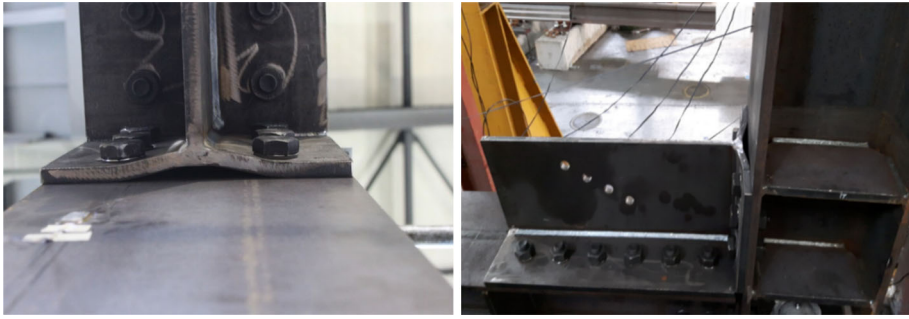


Fig. 25 T-stub connection between gusset plate and column

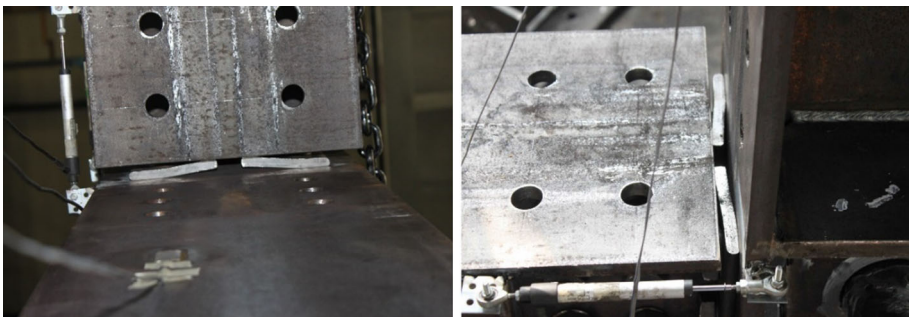


Fig. 26 Web angle connection between beam web-column flange

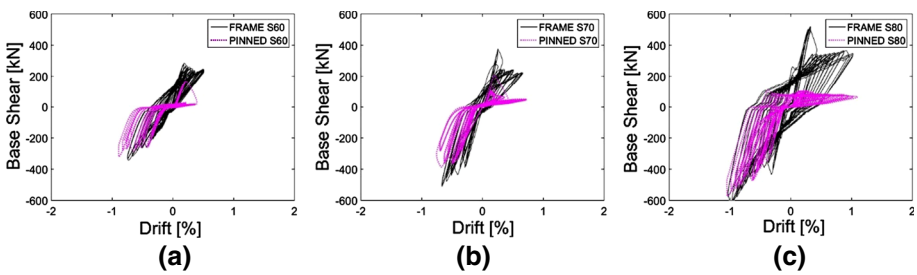


Fig. 27 Global base shear-drift behaviour comparisons of single diagonal MRF and PC frames. a S60-MRF versus S60-PC, b S70-MRF versus S70-PC, c S80-MRF versus S80-PC

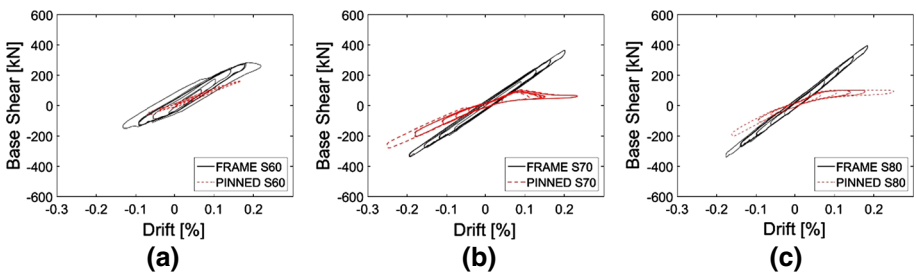


Fig. 28 Initial stiffness comparisons of Single diagonal MRF and PC specimens. a S60, b S70, c S80

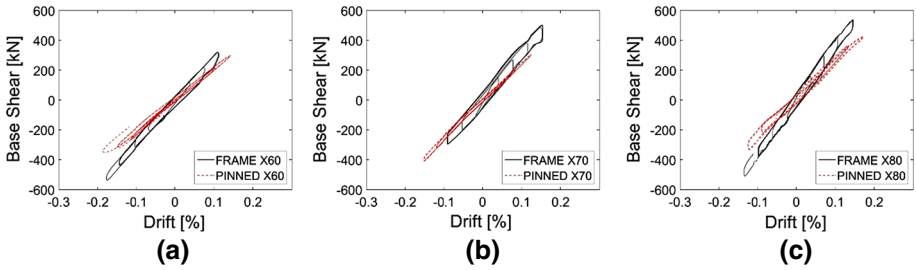


Fig. 29 Initial stiffness comparisons of X-braced MRF and PC specimens. **a** X60, **b** X70, **c** X80

Table 11 Initial stiffness properties of test specimens

	2L60x60x8		2L70x70x7		2L80x80x8	
	K_X	K_S	K_X	K_S	K_X	K_S
MRF	2796	1299	3505	1670	3680	1888
PC _B	2189	999	2505	963	2698	1081
MRF _B	2515	1124	3224	1494	3399	1712
C_{MRF} (%)	10.1	13.5	8.0	10.5	7.6	9.3
$\bar{\lambda}$	1.42	2.85	1.25	2.41	1.09	2.11

- K_X Global stiffness of the X-braced specimen obtained as a ratio of global base shear divided by global interstorey drift at elastic phase, kN/(mm/mm)
- K_S Global stiffness of the single-diagonal specimen obtained as a ratio of global base shear divided by global interstorey drift at elastic phase, kN/(mm/mm)
- MRF Global stiffness values calculated for MRF specimens
- PC_B Global stiffness values calculated for PC specimens
- MRF_B Global stiffness values calculated subtracting the frame stiffness (281 kN/[mm/mm] for X-braced, 176 kN/[mm/mm] for single-bracing specimens) from MRF values
- C_{MRF} Per-cent contribution of frame action on braced frame specimens

Lateral stiffness contribution of the frame action (C_{MRF}) is between 7.6 and 13.5% depending on boundary conditions, and bracing slenderness. PC specimens have lower global initial stiffness values with respect to MRF specimens, with the same bracing profiles, because of their ideally pinned connections.

4 Conclusions

Bracing gusset plate connections, although normally designed as simple pinned connections, indeed develop considerable strength and stiffness. This paper investigated the contribution of this “secondary frame action” to the global behaviour of CBF structures, in the context of moderate seismicity. Extra stiffness and strength provided by gusset plate connections have been evidenced by means of full scale tests. Following observations have been made from the tests:

- Secondary frame resistance combined with the post-buckling resistance of bracings counted between 58 and 80% of the overall braced specimen resistance.
- Following the total failure of bracings at very large inter-storey drifts, secondary frame action provided between 46 and 127% of the resistance previously developed by the overall braced specimen.
- Although the CBF systems are known to have limited ductility, when the frame action is taken into account, the overall ductility reached important values (between 1.73 and 4.99 times the ductility provided by bracings-only). This ductility levels have been reached at the resistance levels between 58 and 80% of the maximum resistance of the braced specimen.
- Lateral stiffness contribution of the secondary frame was between 7.6 and 13.5%, which depended on the boundary conditions, and bracing Sections
- 75% of the elastic stiffness and 79% of the ultimate resistance of the secondary frame, were provided by gusset plate connections. The rest was due to the beam-to-column shear connections.
- PC specimens had lower global initial stiffness values with respect to MRF specimens, with the same bracing profiles. This difference is caused by the ideally pinned connections of PC specimens.

These results suggest that, in moderate seismic regions, performance of CBF systems can be optimized if the frame action provided by gusset plates is explicitly taken into account. Such contribution can be maximized engaging the beam and column by means of a gusset plate connection (instead of other bracing connection types where gusset plates are connected only on the beam), or a similar solution with the aim of increasing the global stiffness, strength, and ductility. This flexural capacity can be further enriched with additional plates, or involving the composite slab action. Such an intermediate effort may let designer to consider an increased ductility, which can enhance the economy of the building project. It should also be underlined that, in this study, gusset plates are designed to remain elastic and buckling-resistant. It is known that, allowing some inelasticity to the gusset plates, the ductility of the CBF systems increase even more (Hsiao et al. 2012).

Furthermore, current design procedure with simple pinned beam-end assumption does not reflect the realistic behavior of concentrically braced frames. This may lead to wrong estimations both at analysis and design stages in terms of global stiffness and strength characteristics of these type of structures. The author is working on a companion paper that will present a numerical case study based on these experimental conclusions, and provide increased global ductility parameters that can be used in design.

Acknowledgements This article presents the results of full scale tests performed within MEAKADO project coordinated by Prof. Herve Degee, which is carried out with the financial grant of the Research Program of the Research Fund for Coal and Steel of the European Commission (RFSR-CT-2013-00022). Special thanks to Prof. Carlo Andrea Castiglioni, for his precious comments. Thanks to the manager and technicians of the LPM laboratories of Politecnico di Milano. Assistance of the Master thesis students Alberto Volonterio and Umberto Rico during the test implementations is also deeply appreciated.

References

- Aboosaber M, Bradley C, Nelson J, Hines EM (2012) Modeling reserve system performance for low ductility braced frames. In T. U. S. o. Engineering (Ed). Tufts University Structural Systems Communication (TUSSC), Medford, MA, pp 122

- American Institute of Steel Construction (2010) Seismic provisions for structural steel buildings. Seismic provisions for structural steel buildings
- BCJ (1997) Structural provisions for building structures. Tokyo (in Japanese)
- Callister JT, Pekelnicky RG (2011) Seismic evaluation of an existing low ductility braced frame building in California. In: Proceedings of ASCE structures congress. ASCE, New York
- Carter CJ (2009) Connections and collapse resistance in $R = 3$ braced frames. PhD thesis
- Degée H et al (2013) Design of steel and composite structures with limited ductility requirements for optimized performances in moderate earthquake areas (MEAKADO Research Proposal for EU-RFCS)
- Degée H, Hoffmeister B, Castiglioni CA, Martin PO, Calderon I (2015) The “MEAKADO” Project: designing steel and composite structures for optimized performances in moderate earthquake areas. In: Eighth international conference on advances in steel structures
- Elghazouli A, Castro JM, Izzuddin BA (2008) Seismic performance of composite moment-resisting frames. *Eng Struct* 30:1802–1819. doi:10.1016/j.engstruct.2007.12.004
- EN 1993-1-1, European Standard (2005) Eurocode 3: Design of steel structures—Part 1-1: General rules and rules for buildings. Eurocode 3, vol 1, p 91
- EN1993-1-1-2005 (2005a) Design of steel structures—Part 1.1: General rules and rules for buildings. European Committee for Standardization, CEN, Brussels
- EN1993-1-1-2005 (2005b) Design of steel structures—Part 1.8: Design of joints. European Committee for Standardization, CEN, Brussels
- EN1998-1-2004 (2004) Design of structures for earthquake resistance—Part 1: General rules, seismic actions and rules for buildings. European Committee for Standardization, CEN, Brussels
- Gioncu V, Mazzolani F (2013) Seismic design of steel structures. CRC Press
- Han S-W, Choi Y-S (2008) Seismic hazard analysis in low and moderate seismic region-Korean peninsula. *Struct Saf* 30:543–558. doi:10.1016/j.strusafe.2007.10.004
- Hines E, Appel M, Cheever P (2009) Collapse performance of low-ductility chevron braced steel frames in moderate seismic regions. *AISC Eng J* 3rd Quarter, 149–180
- Hsiao PC, Lehman DE, Roeder CW (2012) Improved analytical model for special concentrically braced frames. *J Constr Steel Res* 73:80–94. doi:10.1016/j.jcsr.2012.01.010
- Hsiao PC, Lehman DE, Roeder CW (2013) Evaluation of the response modification coefficient and collapse potential of special concentrically braced frames. *Earthq Eng Struct Dyn* 42:1547–1564. doi:10.1002/eqe.2286
- Kanyilmaz A (2015) Inelastic cyclic numerical analysis of steel struts using distributed plasticity approach. COMPDYN 2015. In: 5th ECCOMAS thematic conference on computational methods in structural dynamics and earthquake engineering, National Technical University of Athens, pp 3663–74
- Kanyilmaz A, Castiglioni CA, Degée H, Martin P (2015) A preliminary assessment of slenderness and overstrength homogeneity criteria used in the design of concentrically braced steel frames in moderate seismicity 25–7
- Kelly DJ, Zona JJ (2006) Design tips for steel in low or moderate seismicity regions. *Mod Steel Constr* 46(2):50
- Kishiki S, Yamada S, Wada A (2008) Experimental evaluation of structural behaviour of gusset plate connection in BRB frame system. 14th World conference on earthquake engineering, Beijing, China
- Málaga-Chuquitaype C, Elghazouli AY, Enache R (2014) Contribution of secondary frames to the mitigation of collapse in steel buildings subjected to extreme loads. *Struct Infrastruct Eng* 2479:1–16. doi:10.1080/15732479.2014.994534
- Marino EM, Nakashima M, Mosalam KM (2005) Comparison of European and Japanese seismic design of steel building structures. *Eng Struct* 27:827–840. doi:10.1016/j.engstruct.2005.01.004
- Murty CVR, Malik JN (2008) Challenges of low-to-moderate seismicity in India. In special issue: Earthquake engineering in the low and moderate seismic regions of Southeast Asia and Australia (2008). *EJSE*, 64–78
- Nelson TA, Gryniuk MC, Hines EM (2006) Comparison of low-ductility moment resisting frames and chevron braced frames under moderate seismic demands. *Moment* 2:4
- Pinto PE (2000) Design for low/moderate seismic risk. *Bull NZ Soc Earthq Eng* 33:303–324
- Reaveley LD, Nordenson GJ (1990) Acceptable damage in low and moderate seismic zones. In: Fourth US-Japan workshop on the improvement of building structural design practices, Hawaii
- Stoakes CD (2012) Beam-column connection flexural behavior and seismic collapse performance of concentrically braced frames
- Stoakes C, Fahnestock L (2010) Flexural behavior of concentrically-braced frame beam-column connections. *Structures congress 2010*, pp 1350–1360
- UNI EN 1090-2 (2011) UNI EN 1090-2 Execution of steel structures and aluminium structures Part 2: Technical requirements for steel structures

- Uriz P, Mahin SA (2008) Toward earthquake-resistant design of concentrically braced steel-frame structures. PEER report 2008/08. Earthquake Engineering Research Center, University of California, Berkeley
- Vargas RE, Bruneau M (2008) Experimental validation of the structural fuse concept. In: Proceedings of the 14th world conference on earthquake engineering: innovation practice safety
- Yoo JH, Lehman DE, Roeder CW (2008) Influence of connection design parameters on the seismic performance of braced frames. *J Constr Steel Res* 64:607–623. doi:[10.1016/j.jcsr.2007.11.005](https://doi.org/10.1016/j.jcsr.2007.11.005)
- Yoo JH, Roeder CW, Lehman DE (2009) Simulated behavior of multi-story X-braced frames. *Eng Struct* 31:182–197. doi:[10.1016/j.engstruct.2008.07.019](https://doi.org/10.1016/j.engstruct.2008.07.019)